



Journal Name

COMMUNICATION

Fluorescence of a Chiral Pentaphene Derivative Derived from the Hexabenzocoronene Motif

Received 00th January 20xx,
Accepted 00th January 20xx

Philipp Rietsch,^[a] Jan Soyka,^[a] Steffen Brülls^[d], Jasmin Er,^[a] Katrin Hoffmann,^[b] Julia Beerhues,^[c]
Biprajit Sarkar,^[c] Ute Resch-Genger,^{[b]*} and Siegfried Eigler^{[a]*}

DOI: 10.1039/x0xx00000x

www.rsc.org/

^a M. Sc. Philipp Rietsch, Prof. Dr. Siegfried Eigler; Institute of Chemistry and Biochemistry

Freie Universität Berlin Takustraße 3, 14195 Berlin, Germany.
E-mail: siegfried.eigler@fu-berlin.de

^b Dr. Ute Resch-Genger, Dr. Katrin Hoffmann; Bundesanstalt für Materialforschung und -prüfung (BAM), Department 1, Division Biophotonics, Richard Willstätter Straße 11, 12489 Berlin, Germany, E-Mail: ute.resch@bam.de

^c M. Sc. Julia Beerhues, Prof. Dr. Biprajit Sarkar
Institute of Chemistry and Biochemistry, Freie Universität Berlin, Fabeckstraße 34-36, 14195 Berlin, Germany

^d Chalmers University of Technology SE-412 96 Gothenburg, Sweden

^e Address here.

† Footnotes relating to the title and/or authors should appear here.

Electronic Supplementary Information (ESI) available: [details of any supplementary information available should be included here]. See DOI: 10.1039/x0xx00000x

Table of contents

1. General Information	3
2. Synthetic procedure.....	4
Synthesis of 1-(1-(<i>tert</i> -Butyl)-4-ethynylbenzen)-2,3,4,5,6-(penta-(4- <i>tert</i> -phenyl)benzene (3)	4
Synthesis of 2,5,8,11,14-penta- <i>tert</i> -butyl-18-(4-(<i>tert</i> -butyl)phenyl)dibenzo[fg,ij]pyreno[5,4,3,2,1-pqrst]pentaphene (4).....	5
Hexa- <i>tert</i> -butylhexa- <i>peri</i> -hexabenzocoronene (5)	7
2-((4-methoxyphenyl)ethynyl)-1,1'-biphenyl (6).....	7
9-(4-methoxyphenyl)phenanthrene (7).....	8
3. Crystal structure	10
4. UV/Vis and fluorescence measurements.....	13
5. Fluorescence lifetimes measurements	17
6. Solid state fluorescence measurements.....	18
7. Computational Study of the racemization barrier.....	21

1. General Information

All reagents were purchased from commercial sources and used without further purification. Dry solvents were purchased from Acros Organics. ALUGRAM Xtra SIL G/UV₂₅₄ plates by Macherey-Nagel were used for thin-layer chromatography. Isolation of products by chromatography was performed with silica from Macherey-Nagel Silica 60 M (0.04-0.063 mm). NMR spectra were recorded on a JOEL ECX 400 (¹H 400 MHz, ¹³C 101 MHz), JEOL Eclipse+ 500 (¹H 500 MHz, ¹³C 126 MHz) and BRUKER AVANCE 700 (¹H 700 MHz, ¹³C 176 MHz) spectrometer at 25 °C. The chemical shifts δ are calibrated on the respective solvent peak as internal standard. All shifts are reported in ppm and NMR multiplicities are abbreviated as s (singlet), d (duplet), t (triplet), m (multiplet). Coupling constants *J* are reported in Hz. UV/Vis spectra were recorded on a Cary 50 Bio photospectrometer (Varian). Fluorescence spectra were recorded on a LS 50 B luminescence spectrometer from PerkinElmer. UV/Vis and Fluorescence spectra were measured in quartz glass cuvettes with 1 cm path length. IR Spectra were recorded on a FT/IR 4100 spectrometer from JASCO. Elemental analysis was performed on an VARIO EL from Elementar.

Single crystals suitable for X-ray diffraction analysis were grown by slow evaporation from chloroform and methanol (9:1). X-ray data were collected on a Bruker D8 Venture system at 100(2) K using graphite-monochromated Mo_{K α} radiation ($\lambda = 0.71073$ Å). The strategy for the data collection was evaluated using APEX3 software and the data were collected by the omega + phi scan techniques. The data were scaled and reduced using SAINT+ and SADABS software. The structure was solved by intrinsic phasing using SHELXT-2014/7. It was refined by full matrix least-squares using SHELXL-2014/7 and was refined on *F*². Non-hydrogen atoms were refined anisotropically.^[1-7] CCDC (1923092) contains the supplementary crystallographic data for this paper.

Photoluminescence quantum yields (Φ) were determined absolutely with an integrating sphere setup from Hamamatsu (Quantaaurus-QY C11347-11). All Φ measurements were performed at 25 °C using special 10 mm x 10 mm long neck quartz cuvettes from Hamamatsu. The fluorescence lifetime (*t*), the average time in which the fluorophore is in an excited state before it relaxes to the ground state, was recorded on a fluorometer FLS 920 (Edinburgh Instruments) equipped with a Hamamatsu R3809U-50 (range 200–850 nm, response width <25 ps), Multi-Channel Plate (MCP) detector, Czerny-Turner double monochromators and either a supercontinuum laser (Fianium SC400-2-PP) or a Edinburgh Instrument EPLED-330 (picosecond pulsed light emitting diode) for excitation at 375 nm, or a Edinburgh Instrument EPL-375 (picosecond pulsed diode laser) for excitation at 330 nm. All the measurements were performed at *T* = 298 K using 10 mm x 10 mm quartz cuvettes from Hellma GmbH always filled with 2 mL of solvent or dye solution. Before each measurement, the instrument response function (IRF) was measured. The lifetime measurements were analysed with Edinburgh Instruments FAST Software and fitted with a deconvolution fit. All the lifetimes could be evaluated mono, bi- or tri-exponentially with a reduced *X*² between 0.8 and 3.0.

The fluorescence spectra of the crystals in the solid state and microscopic images were recorded with an Olympus FluoView FV1000 (Olympus GmbH, Hamburg, Germany). For UV excitation, a DPSS Cobolt Zouk® (355 nm; 10 mW), and for transmission imaging an additional multiline argon ion laser (30 mW, 488 nm) were used as excitation sources, which were reflected by a beamsplitter (BS 20/80) and focused onto the sample through an Olympus objective UPLSAPO 10X (numerical aperture N.A. 0.40). The emitted photons were recollimated with the same objective and focused onto a PMT. Emission signals were detected in a wavelength range between 460 nm and 700 nm with spectral resolution of 5 nm and a step width of 2 nm. The spatial resolved fluorescence spectra are raw spectra, not specifically corrected for the wavelength-dependent spectral responsivity of the detection system of the microscope.

2. Synthetic procedure

Synthesis of 1-(1-(*tert*-Butyl)-4-ethynylbenzen)-2,3,4,5,6-(penta-(4-*tert*-phenyl)benzene (**3**)

The synthesis of **3** was done as depicted in Figure S1. All procedures and analytic results of compounds **1**, **2** and **8-12** were in accordance with the literature.^[8-9] The reaction description below is for the Diels-Alder reaction leading to compound **3**.

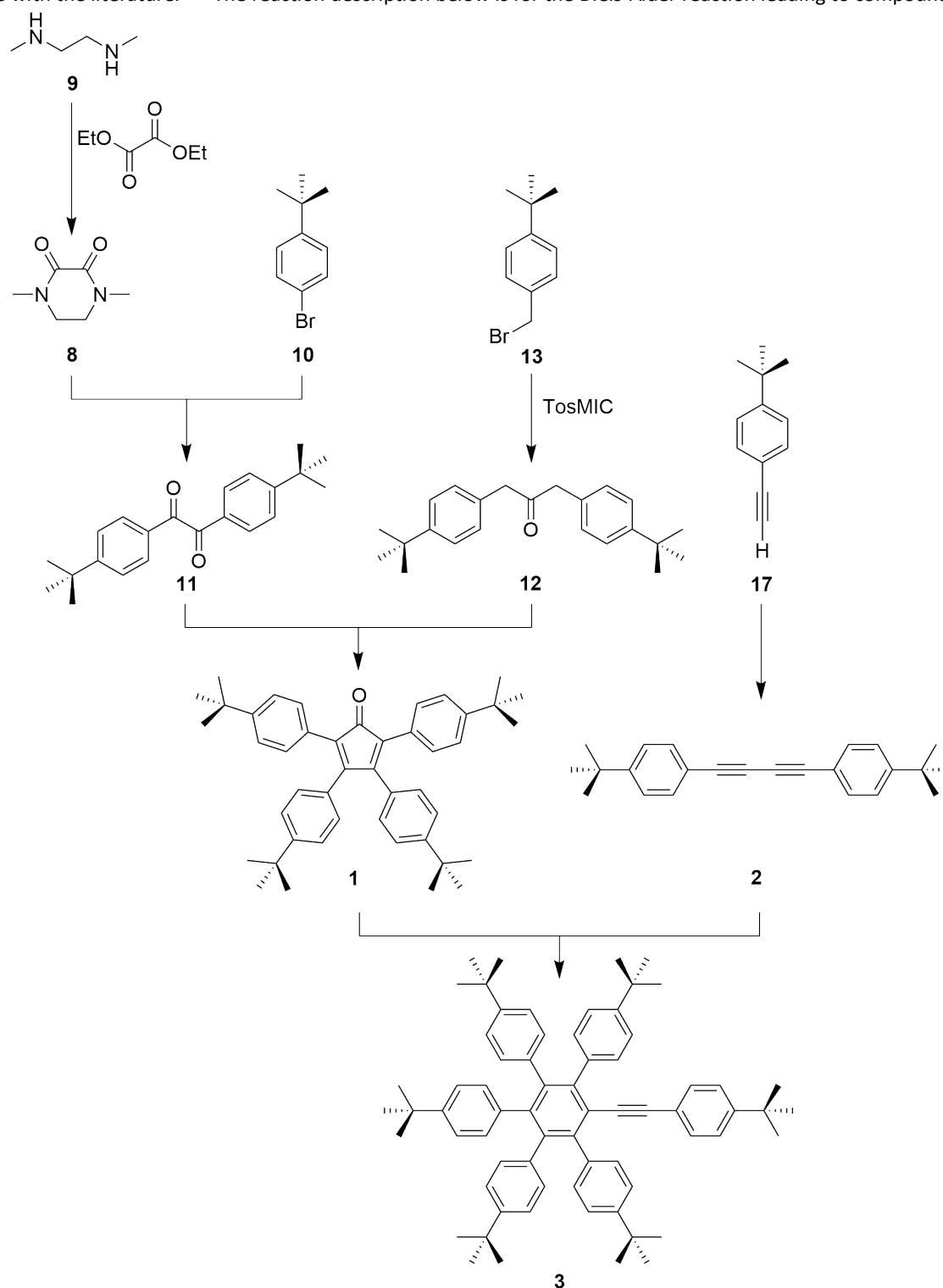


Figure S1: Synthetic route towards hexaarylbenzene derivative **3**.

2,3,4,5-Tetrakis(4-(*tert*-butyl)phenyl)cyclopenta-2,4-dien-1-one (0.249 g, 0.41 mmol, 0.95 eq.) **1** and 1,4-Bis(4-(*tert*-butyl)phenyl)buta-1,3-diyne (0.121 g, 0.38 mmol, 1.0 eq) **2** were dissolved in diphenyl ether (2 mL) under argon atmosphere. The solution was stirred at 250 °C for 24 hours. The red solution was cooled to RT, DCM (5 mL) and subsequently methanol (75 mL) were added. A colorless precipitate formed which was filtered and washed with cold methanol (3x 5 mL). The raw product was purified by column chromatography (SiO₂, hexane/DCM, 7:1). After drying, 1-(1-(*tert*-butyl)-4-ethynylbenzen)-2,3,4,5,6-(penta-(4-*tert*-phenyl)benzene was yielded as a colorless solid (0.24 mmol, 0.216 g, 59%)

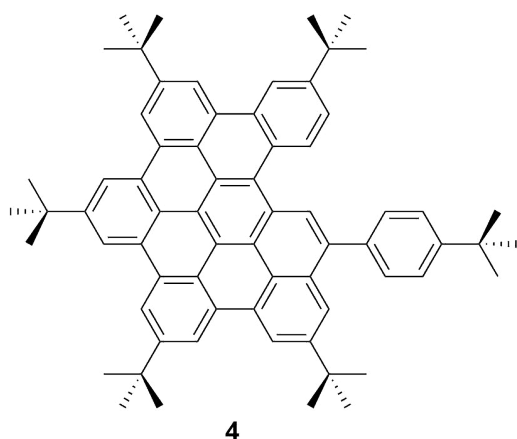
¹H-NMR (700 MHz, CDCl₃): δ [ppm] = 1.09 (s, 9H, *t*-Bu), 1.11 (s, 18H, *t*-Bu), 1.22 (s, 9H, *t*-Bu), 1.29 (s, 18H, *t*-Bu), 6.62 – 6.64 (d, $J_{H,H}$ = 8.4 Hz, 2H, Ar), 6.66 – 6.68 (d, $J_{H,H}$ = 8.4 Hz, 2H, Ar), 6.72 – 6.74 (d, $J_{H,H}$ = 8.0 Hz, 4H, Ar), 6.80 – 6.82 (d, $J_{H,H}$ = 8.4 Hz, 2H, Ar), 6.84 – 6.86 (d, $J_{H,H}$ = 8.0 Hz, 4H, Ar), 7.07 – 7.09 (d, $J_{H,H}$ = 8.4 Hz, 2H, Ar), 7.16 – 7.20 (m, 17H, Ar)

¹³C-NMR (175 MHz, CDCl₃): δ [ppm] = 31.26 (*t*-Bu), 31.31 (*t*-Bu), 31.33 (*t*-Bu), 31.54 (*t*-Bu), 34.20 (Ar-C(Me)₃), 34.23 (Ar-C(Me)₃), 34.53 (Ar-C(Me)₃), 34.74 (Ar-C(Me)₃), 96.60 (Ar-C≡C-Ar), 89.79 (Ar-C≡C-Ar), 121.14 (Ar), 122.80 (Ar), 123.23 (Ar), 123.33 (Ar), 123.73 (Ar), 124.84 (Ar), 130.74 (Ar), 130.98 (Ar), 131.02 (Ar), 131.11 (Ar), 137.33 (Ar), 137.57 (Ar), 137.95 (Ar), 140.44 (Ar), 137.57 (C Ar), 137.95 (Ar), 140.44 (Ar), 141.48 (Ar), 143.14 (Ar), 147.77 (Ar), 147.88 (Ar), 148.72 (Ar), 150.76 (Ar).

MS (EI): m/z = 894.53 [M⁺] (calc. 894.61).

EA [%]: C: 89.99 (calc. 91.22), H: 8.86 (calc. 8.78).

Synthesis of 2,5,8,11,14-penta-*tert*-butyl-18-(4-(*tert*-butyl)phenyl)dibenzo[fg,ij]pyreno[5,4,3,2,1-pqrst]pentaphene (**4**)



Under argon atmosphere compound **3** (0.1004 g, 0.112 mmol, 1.0 eq.) was dissolved in DCM (50 mL) and cooled to 0 °C. A solution of pre-dried iron (III) chloride (0.218 g, 1.344 mmol, 12.0 eq.) in freshly distilled nitromethane (5 mL) was added dropwise. The solution was then stirred for 1 hour at 0 °C and subsequent stirring for 15 hours at RT. The red solution was then quenched with methanol (50 mL) which gave a yellow suspension. Water (50 mL) was added and extracted with DCM (3x 50 mL). The organic phases were combined, dried, evaporated, and dried. The resulting crude product was purified by column chromatography (SiO₂, hexane/DCM, 8:1) to yield a yellow solid (0.079 g, 0.090 mmol, 80%).

¹H-NMR (700 MHz, CDCl₃): δ [ppm] = 1.51 (s, 9H, *t*-Bu), 1.64 (s, 9H, *t*-Bu), 1.66 (s, 9H, *t*-Bu), 1.78 (s, 9H, *t*-Bu), 1.81 (s, 9H, *t*-Bu), 1.82 (s, 9H, *t*-Bu), 7.68 – 7.69 (d, $J_{H,H}$ = 8.4 Hz, 2H, Ar), 7.81 – 7.85 (d, $J_{H,H}$ = 8.4 Hz, 2H, Ar), 7.86–7.87 (m, 1H, Ar), 8.51 (s, 1H, Ar), 8.93 (s, 1H, Ar), 9.08 (s, 1H, Ar), 9.16 – 9.20 (m, 3H, Ar), 9.26 – 9.29 (m, 4H, Ar), 9.37 (s, 1H, Ar).

¹³C-NMR (175 MHz, CDCl₃): δ [ppm] = 150.49, 149.76, 149.33, 149.19, 149.11, 148.87, 138.87, 138.15, 131.37, 130.87, 130.75, 130.65, 130.58, 130.47, 130.29, 130.27, 130.16, 128.45, 128.40, 125.58, 124.60, 124.48, 124.34, 124.25, 123.98, 123.72, 123.58, 122.46, 122.10, 122.07, 121.00, 120.15, 119.96, 119.25, 119.06, 118.97, 118.90, 118.38, 118.09, 35.87, 35.79, 35.37, 34.93, 32.16, 32.14, 32.07, 31.76, 31.70

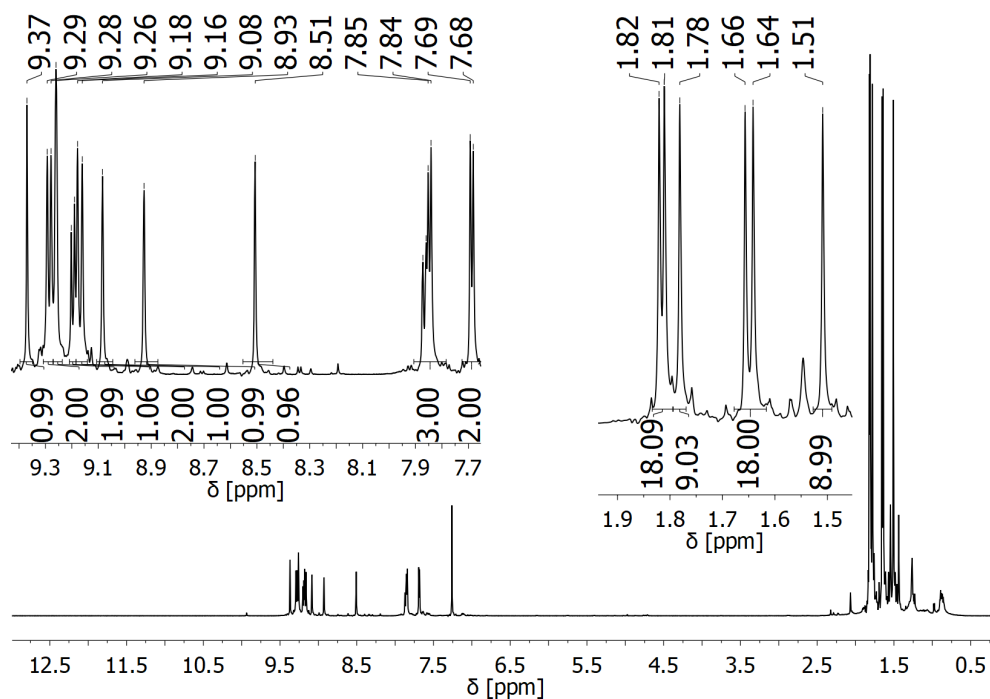
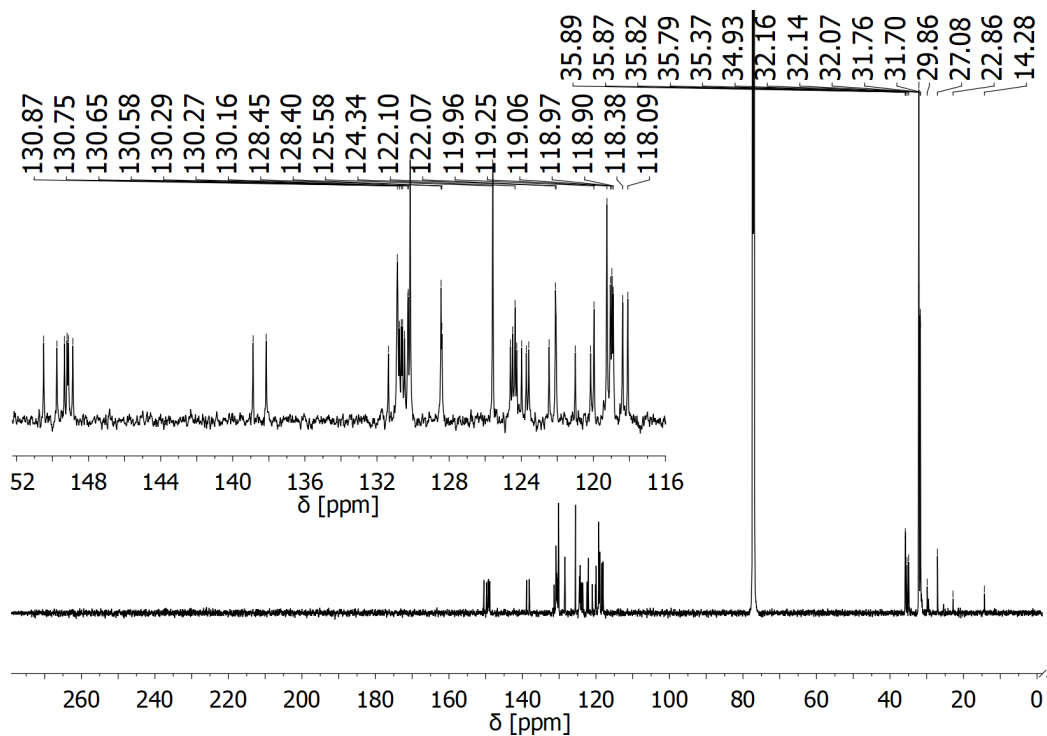
MS (EI): m/z = 886.52 [M⁺] (calc. 886.548).

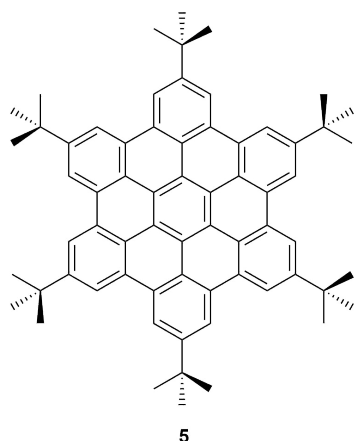
EA [%]: C: 92.04 (calc. 92.05), H: 7.98 (calc. 7.95).

UV/Vis (cyclohexane) λ_{max} nm (ϵ [Lmol⁻¹ cm⁻¹]): 226 (122706), 316 (34272), 350 (64773), 365 (67839), 400 (29242), 424 (32072)

UV/Vis (dichloromethane) λ_{max} nm (ϵ [Lmol⁻¹ cm⁻¹]): 250 (55670), 319 (30149), 353 (56649), 367 (61120), 404 (26447), 427 (28945)

UV/Vis (ethanol) λ_{max} nm (ϵ [Lmol⁻¹ cm⁻¹]): 229 (42468), 316 (22190), 349 (37410), 364 (38458), 400 (18163), 423

Figure S2: ^1H -NMR spectrum of compound **4** recorded on BRUKER AVANCE 700 in CDCl_3 .Figure S3: ^{13}C -NMR spectrum of compound **4** recorded on BRUKER AVANCE 700 in CDCl_3 .

Hexa-*tert*-butylhexa-*peri*-hexabenzocoronene (5)

5

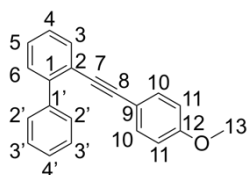
Compound 5 was synthesized by a one pot reaction of hexaphenylbenzene and *t*-BuCl with FeCl₃ acting as oxidant and Lewis acid catalyst. The reaction and analytical data were in accordance with the literature.^[10]

UV/Vis (cyclohexane) λ_{max} nm (ϵ [Lmol⁻¹ cm⁻¹]): 229 (64097), 243 (42147), 364 (50680), 389 (17632)

UV/Vis (dichloromethane) λ_{max} nm (ϵ [Lmol⁻¹ cm⁻¹]): 231 (167666), 240 (128816), 343 (81265), 360 (181660), 390 (58991)

UV/Vis (ethanol) λ_{max} nm (ϵ [Lmol⁻¹ cm⁻¹]): 229 (48901), 242 (33511), 347 (20118), 363 (40746), 395 (11160)

2-((4-methoxyphenyl)ethynyl)-1,1'-biphenyl (6)



Under argon atmosphere, PdCl₂(PPh₃)₂ (0.11 g, 0.15 mmol, 0.21 eq.), 2-iodobiphenyl (0.13 ml, 0.71 mmol, 1.00 eq.) and CuI (0.04 g, 0.21 mmol, 0.30 eq.) were stirred in triethylamine (15 mL). 4-Methoxyphenylacetylene (0.10 mL, 0.73 mmol, 1.03 eq.) was added dropwise. The black suspension was stirred for 24 hours at RT and for 5 hours at 55 °C. After cooling to RT, the suspension was filtered and purified by column chromatography (SiO₂; pentane / ethylacetate, 30:1) to yield 0.05 g (0.18 mmol, 25% yield) of a colourless liquid.

¹H-NMR (500 MHz, CDCl₃): δ [ppm] = 7.70-7.63 (m, 3H, H-3, H-4, H-6), 7.49-7.31 (m, 6H, H-5, H-2', H-3', H-4'), 7.28 (d, ³*J* = 8.7 Hz, 2H, H-10), 6.83 (d, ³*J* = 8.7 Hz, 2H, H-11), 3.80 (s, 3H, H-13).

¹³C-NMR (125 MHz, CDCl₃): δ [ppm] = 159.66 (C-12), 143.77 (C-1), 140.83 (C-1'), 132.93 (C-10), 132.73 (C-3), 129.57 (C-3'), 128.29 (C-5), 127.98 (C-2'), 127.52 (C-4'), 127.16 (C-6), 122.07 (C-4), 120.04 (C-2), 115.76 (C-9), 114.06 (C-11), 92.41, (C-8), 88.23 (C-7), 55.41 (C-13).

MS (ESI): *m/z* = 323.08 (100) [M-K]⁺, 307.10 (60) [M-Na]⁺, 285.12 (35) [M-H]⁺.

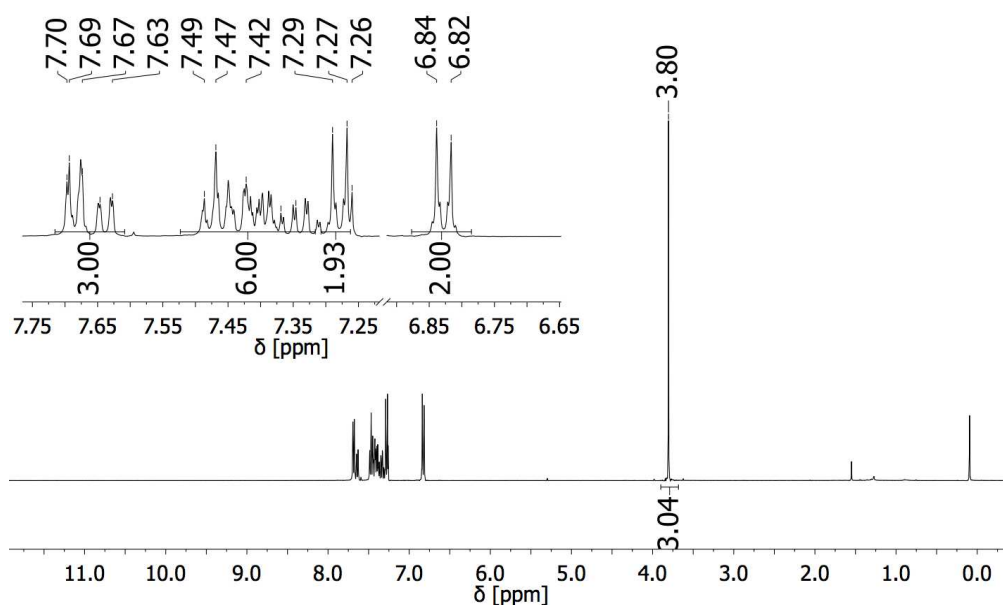


Figure S4: ¹H-NMR spectrum of compound 6 recorded on BRUKER AVANCE III 500 in CDCl₃.

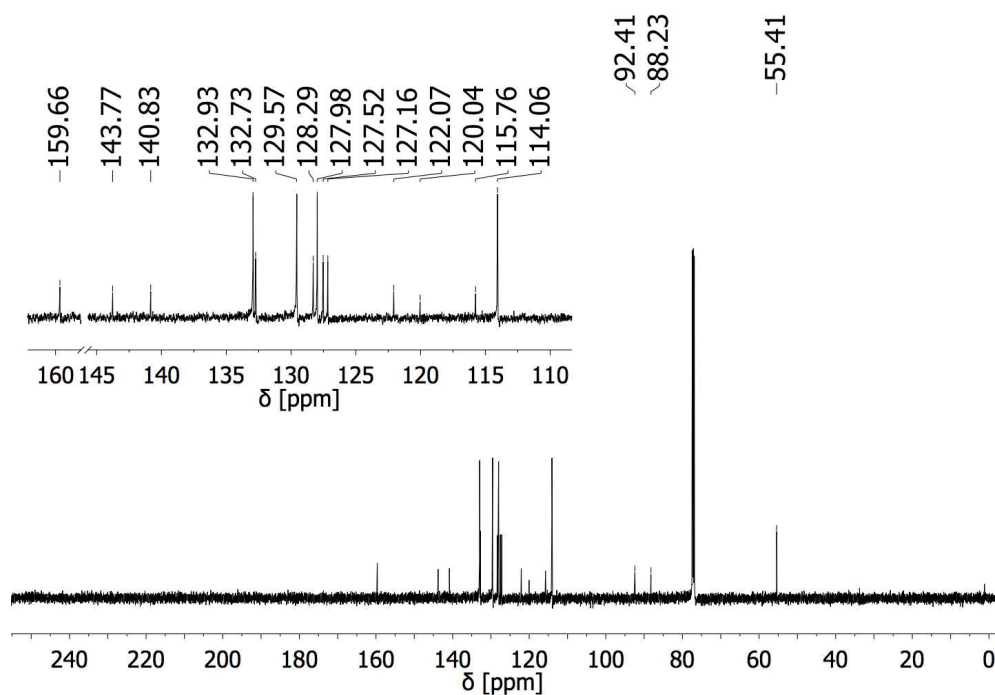
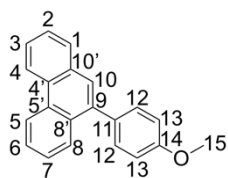


Figure S5: ^{13}C -NMR spectrum of compound 6 recorded on BRUKER AVANCE III 500 in CDCl_3 .

9-(4-methoxyphenyl)phenanthrene (7)

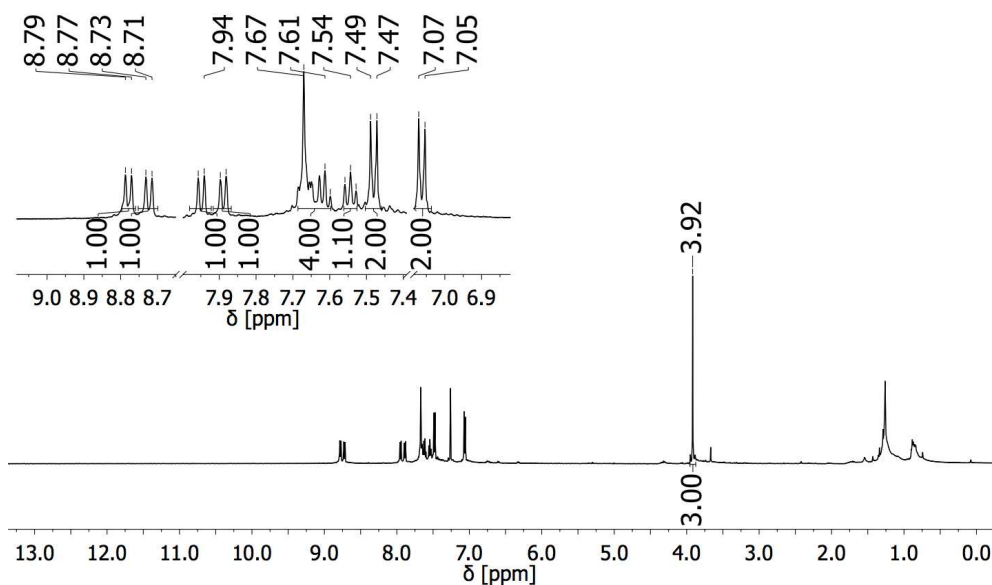
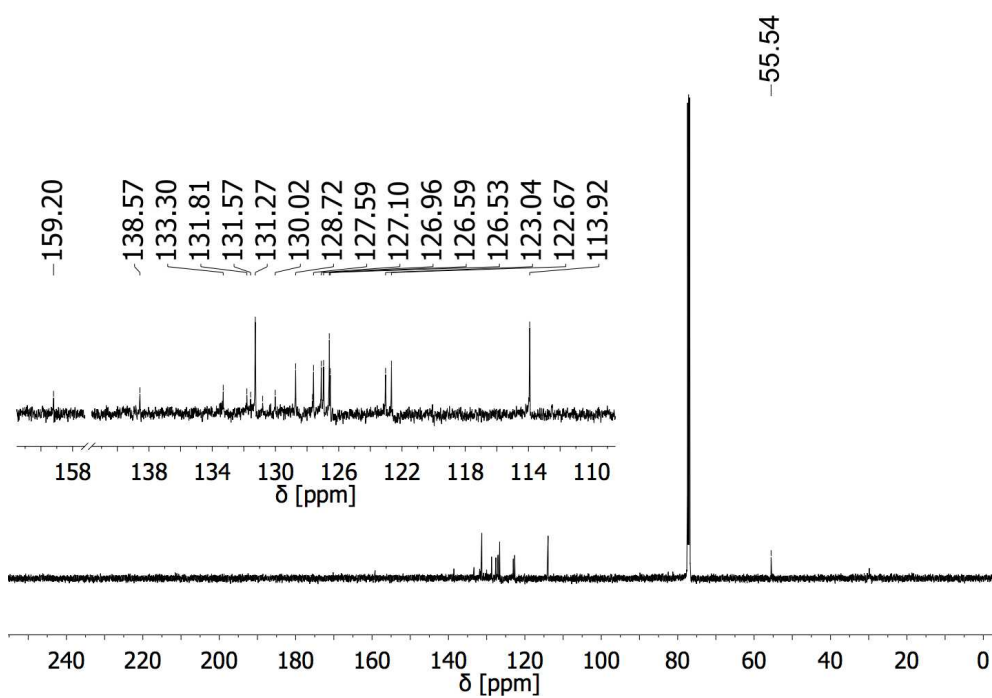


Under argon atmosphere, FeCl_3 (0.02 g, 0.14 mmol, 0.88 eq.) was stirred in dry DCM (50 mL). 2-((4-methoxyphenyl)ethynyl)-1,1'-biphenyl (**6**) (0.045 g, 0.16 mmol, 1.00 eq.) was added dropwise to the black-green solution and stirred at RT. Controlling the reaction procedure by TLC, the reaction was quenched by the addition of methanol (5 mL). The suspension was filtered and the raw solution was purified by column chromatography (SiO_2 ; pentane \rightarrow ethylacetate) to yield 9-(4-methoxyphenyl)phenanthrene as a brownish solid (0.032 g, 0.11 mmol, 69%).

$^1\text{H-NMR}$ (500 MHz, CDCl_3): δ [ppm] = 8.78 (d, $^3J = 8.0$ Hz, 1H, H-5), 8.73 (d, $^3J = 8.0$ Hz, 1H, H-4), 7.95 (d, $^3J = 8.9$ Hz, 1H, H-8), 7.89 (d, $^3J = 8.9$ Hz, 1H, H-1), 7.67-7.60 (m, 4H, H-3, H-6, H-7, H-10), 7.55 (t, $^3J = 7.5$ Hz, 1H, H-2), 7.48 (d, $^3J = 8.5$ Hz, 2H, H-12), 7.07 (d, $^3J = 8.5$ Hz, 2H, H-13), 3.92 (s, 3H, H-15).

$^{13}\text{C-NMR}$ (125 MHz, CDCl_3): δ [ppm] = 159.20 (C-14), 138.57 (C-11), 133.30 (C-10'), 131.81 (C-9), 131.57 (C-5'), 131.27 (C-4'), 130.81 (C-12), 130.02 (C-8'), 128.72 (C-8), 127.65 (C-1), 127.59 (C-7), 127.10 (C-6), 126.96 (C-2), 126.59 (C-3), 126.53 (C-5), 123.04 (C-4), 122.67 (C-10), 113.92 (C-13), 55.54 (C-15).

MS (EI): $m/z = 284.12$ [M] $^+$, 285.12 [M-H] $^+$.

Figure S6: ¹H-NMR spectrum of compound 7 recorded on BRUKER AVANCE III 500 in CDCl₃.Figure S7: ¹³C-NMR spectrum of compound 7 recorded on BRUKER AVANCE III 500 in CDCl₃.

3. Crystal structure

Single crystals of **4** were grown in a mixture of chloroform and methanol (9:1) by slow evaporation. For the comparison of the structures, the crystallographic data of **5** were taken from literature.^[11]

Table S1: Crystallographic data and structure refinement details of compound 5.

Empirical formula	C ₃₄ H ₃₅
Formula weight	443.62
Temperature/K	104(2)
Crystal system	triclinic
Space group	P-1
a/Å	11.0477(12)
b/Å	16.493(3)
c/Å	16.663(3)
α/°	109.226(4)
β/°	102.182(4)
γ/°	108.712(4)
Volume/Å ³	2539.4(7)
Z	4
ρ _{calc} /cm ³	1.160
μ/mm ⁻¹	0.065
F(000)	956.0
Crystal size/mm ³	0.32 × 0.29 × 0.02
Radiation	MoKα (λ = 0.71073)
2θ range for data collection/°	4.674 to 50.802
Index ranges	-13 ≤ h ≤ 12, -19 ≤ k ≤ 19, -20 ≤ l ≤ 20
Reflections collected	72902
Independent reflections	9328 [R _{int} = 0.1009, R _{sigma} = 0.0490]
Data/restraints/parameters	9328/0/631
Goodness-of-fit on F ²	1.024
Final R indexes [I >= 2σ (I)]	R ₁ = 0.0516, wR ₂ = 0.1131
Final R indexes [all data]	R ₁ = 0.0895, wR ₂ = 0.1302
Largest diff. peak/hole / e Å ⁻³	0.27/-0.26

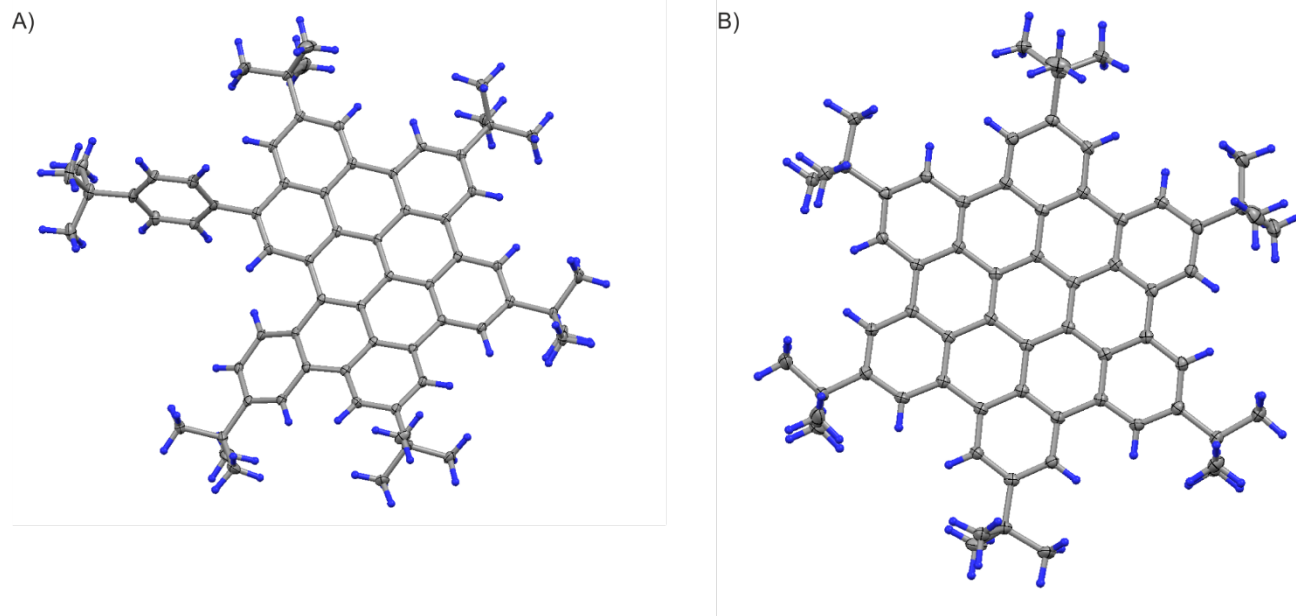


Figure S8: Crystal structures of 4 (A) and 5 (B). The thermal ellipsoids are shown in 50% probability.

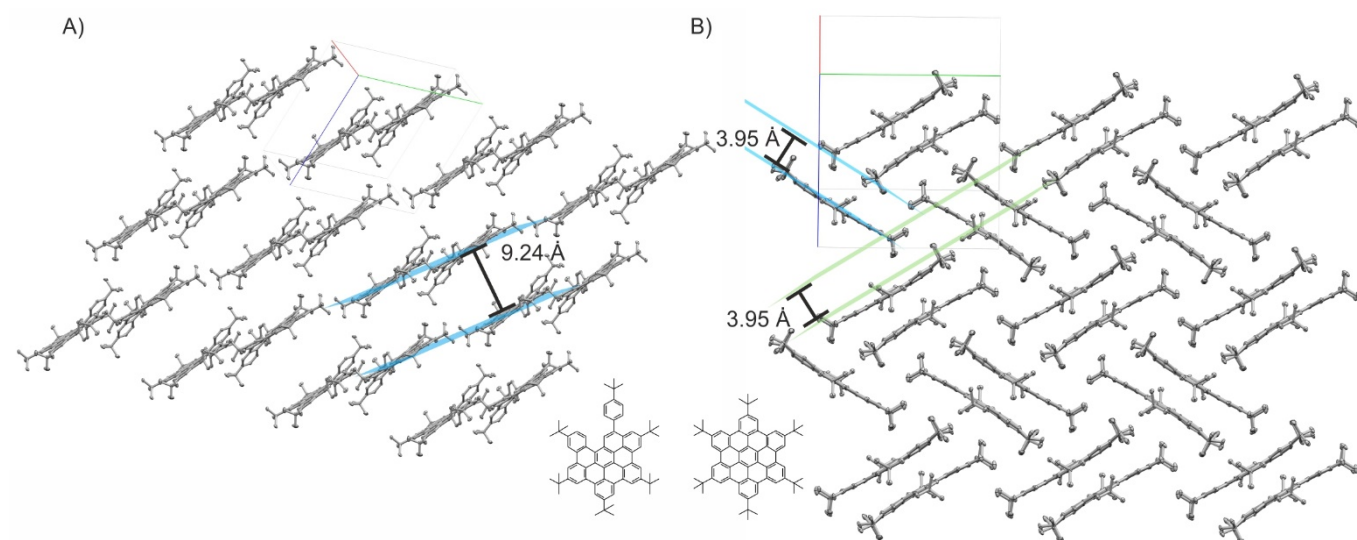


Figure S9: Molecular planes in compound **4** (A) and compound **5** (B). For **5**, the herringbone structure is clearly visible and the interplanar distance is below 4 Å. The interplanar distance of **4** is 9.24 Å. The crystallographic data of **5** was taken from reference^[11]. The unit cell is depicted through the red (direction a), green (direction b) and blue (direction c) lines forming a cube. The depiction of **5** was 1 unit cell in a direction, 4 unit cells in b direction and 3 unit cells in c direction.

4. UV/Vis and fluorescence measurements

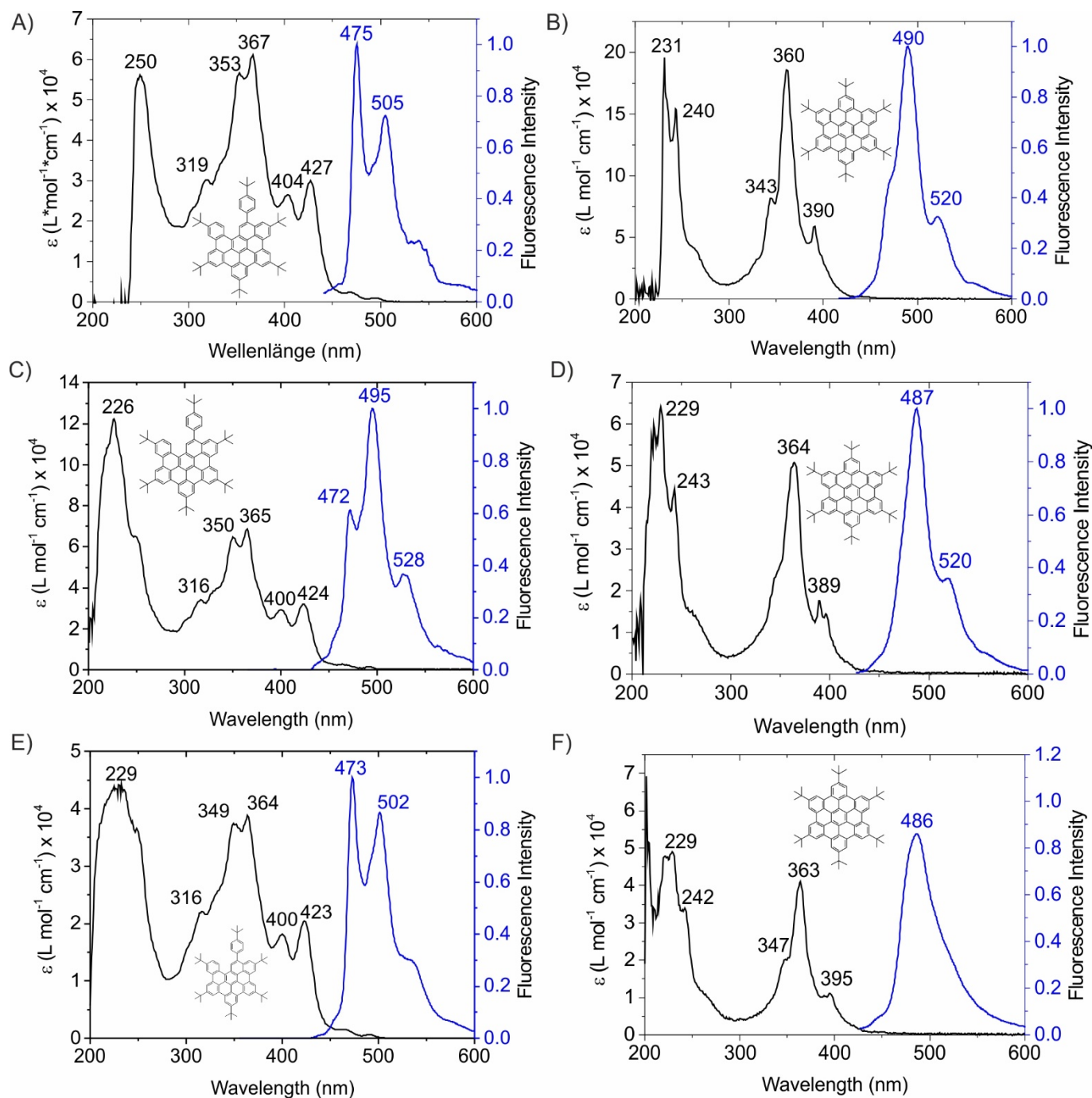


Figure S10: Absorption spectra (black) and fluorescence spectra (blue) of compound 4 (left side) and compound 4 (right side) respectively in dichloromethane (A and B), cyclohexane (C and D) and ethanol (E and F). The excitation wavelength was always chosen near the absorbance maximum about 350 nm. The numbers in the panels without unit refer to the respective absorption (black) and emission maxima (blue) on a wavelength scale. For a more detailed information on the excitation wavelength-s dependent fluorescence see Figure S11 and Figure S12.

Table S2: Absorption Maxima and emission maxima of **4** and **5** with the stokes shift calculated from the respective absorption maxima about 350 nm and emission maxima, both marked with * and written in italic.

	Absorption Maxima		Emission Maxima		Stokes Shift*	
	4	5	4	5	4	5
DCM	250 319 353 <i>367*</i> 404 427	231 240 343 <i>360*</i> 390	<i>475*</i> 505	<i>490*</i> 520	108	130
CH	226 316 350 <i>365*</i> 400 424	229 243 <i>364*</i> 389	472 <i>495*</i> 528	<i>487*</i> 520	130	123
EtOH	229 316 349 <i>364*</i> 400 423	229 242 347 <i>363*</i> 395	<i>473*</i> 502	<i>486*</i>	109	123

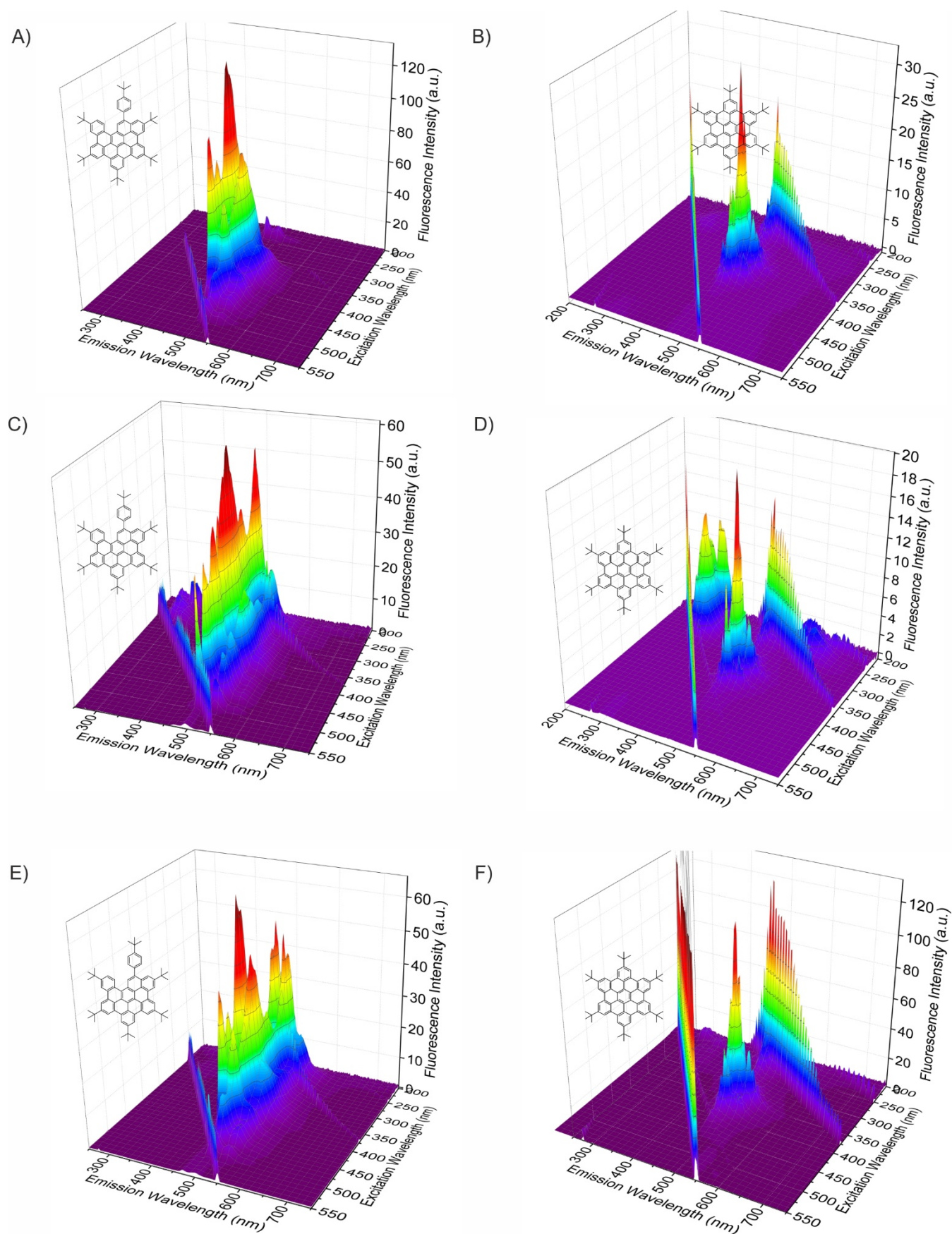


Figure S11: 3D fluorescence maps of **4** (left side) and **5** (right side) respectively. Solvents were dichloromethane in A and B, cyclohexane in C and D and ethanol in E and F. Red areas represent the highest fluorescence (normalized to 1), blue areas no fluorescence. The measurement conditions (slit widths, sensitivity, concentration) were kept constant. The intensity ratio of excitation lamp peak (diagonal lines) to the molecule peaks thus indicates the difference in fluorescence of **4** and **5**.

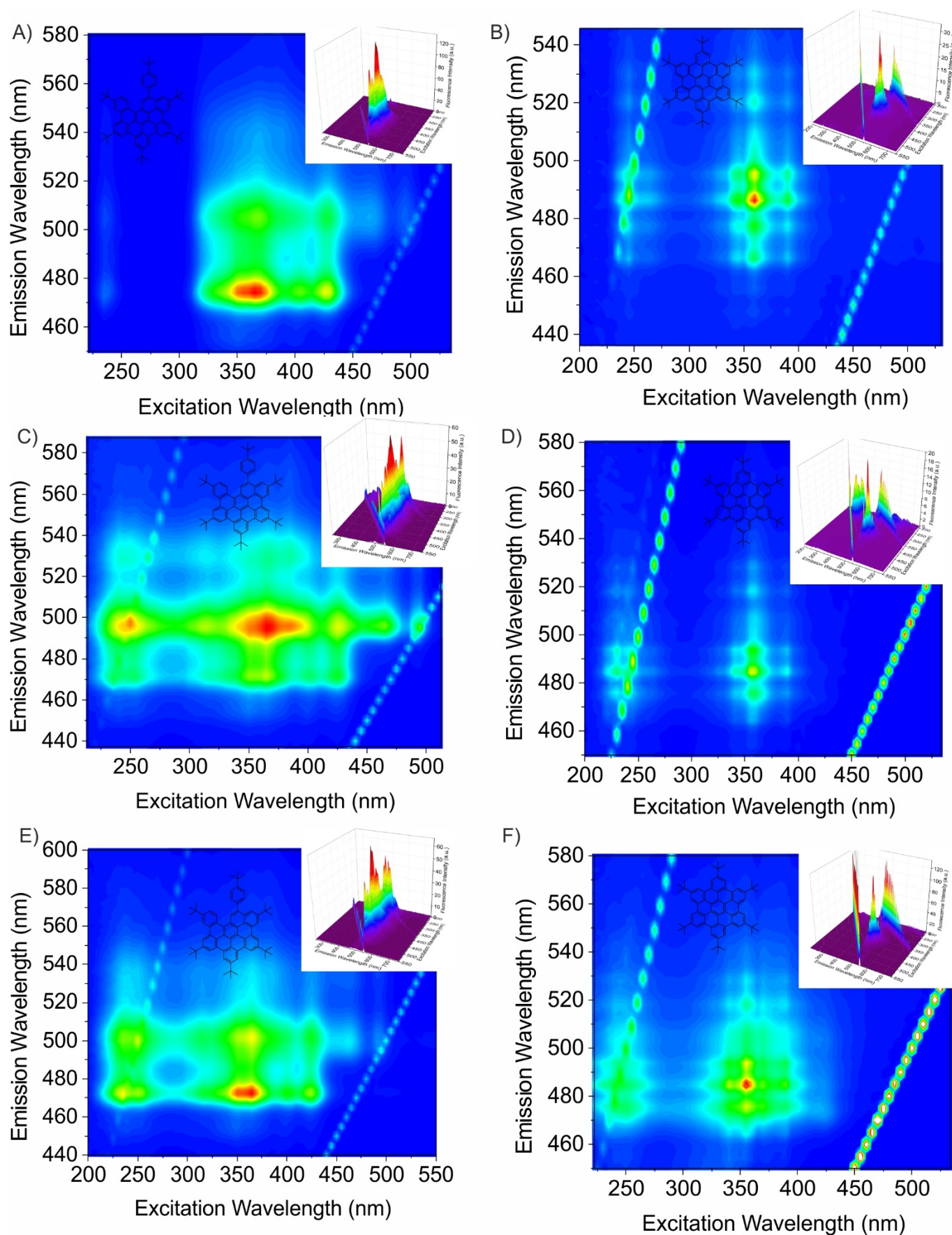


Figure S12: 2D fluorescence maps and 3D fluorescence maps (Insets) of **4** (left side) and **5** (right side) respectively. Solvents were dichloromethane in A and B, cyclohexane in C and D and ethanol in E and F. Red areas represent the highest fluorescence (normalized to 1), blue areas no fluorescence. The intensity ratio of excitation lamp peak (diagonal lines) to the molecule peaks thus indicates the difference in fluorescence of **4** and **5**.

5. Fluorescence lifetimes measurements

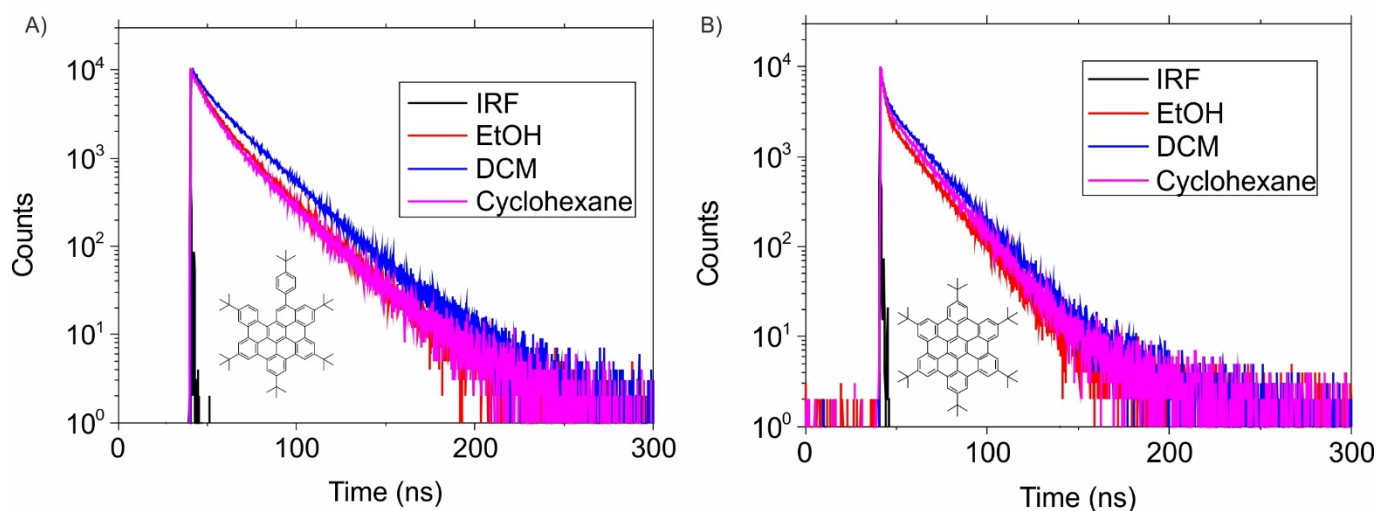


Figure S13: Fluorescence lifetimes of **4** (left side) and **5** (right side) in EtOH (red), DCM (blue) and cyclohexane (pink). Compound **4** was excited at 375 nm and the emission was measured at 490 nm. Compound **5** was excited at 375 nm and the emission was measured at 480 nm.

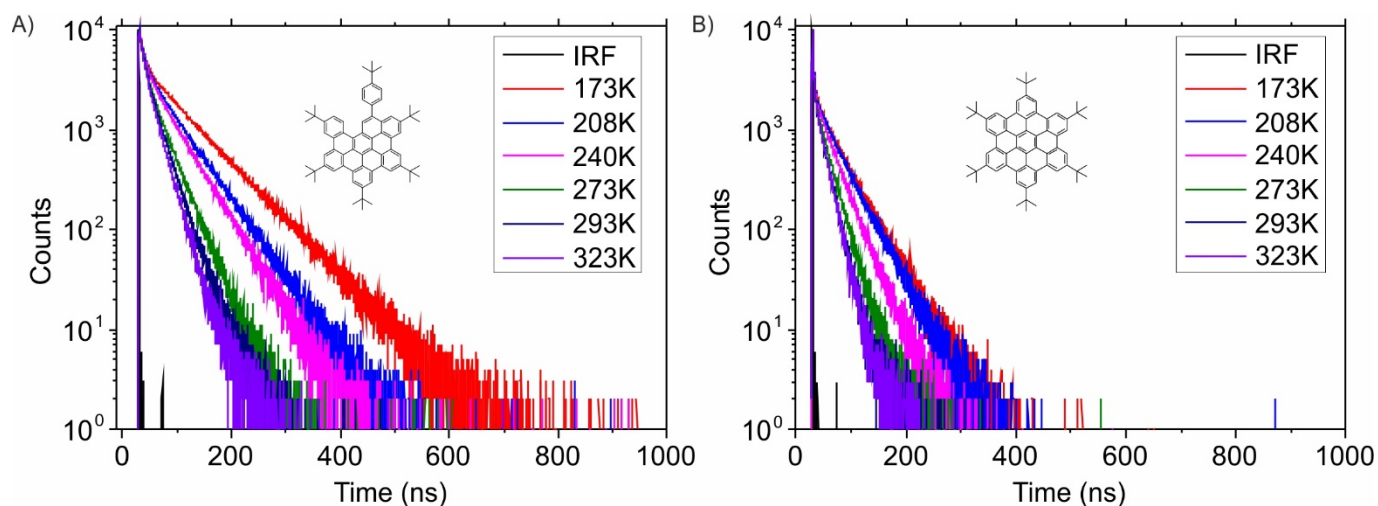


Figure S14: Fluorescence lifetimes of **4** (left side) and **5** (right side) in EtOH at different temperatures from -100 °C to 50 °C. The fluorescence lifetime of **5** decreases from 173K = 27.7 ns to 293K = 11.2 ns. The lifetime of **4** decreases from 63.2 ns at 173K to 20.39 at 293K (18.0 ns at 323K). Compound **4** was excited at 375 nm and the emission was measured at 490 nm. Compound **5** was excited at 375 nm and the emission was measured at 480 nm.

Table S3: Mean fluorescence lifetimes of **4** and **5** in EtOH measured at different temperatures from 50 °C to -100 °C.

	Compound 4	Compound 5
Temperature	τ [ns]	τ [ns]
173K	63.23	27.67
208K	44.09	23.62
240K	36.20	18.07
273K	24.00	11.83
293K	20.39	11.15
323K	18.02	7.93

6. Solid state fluorescence measurements

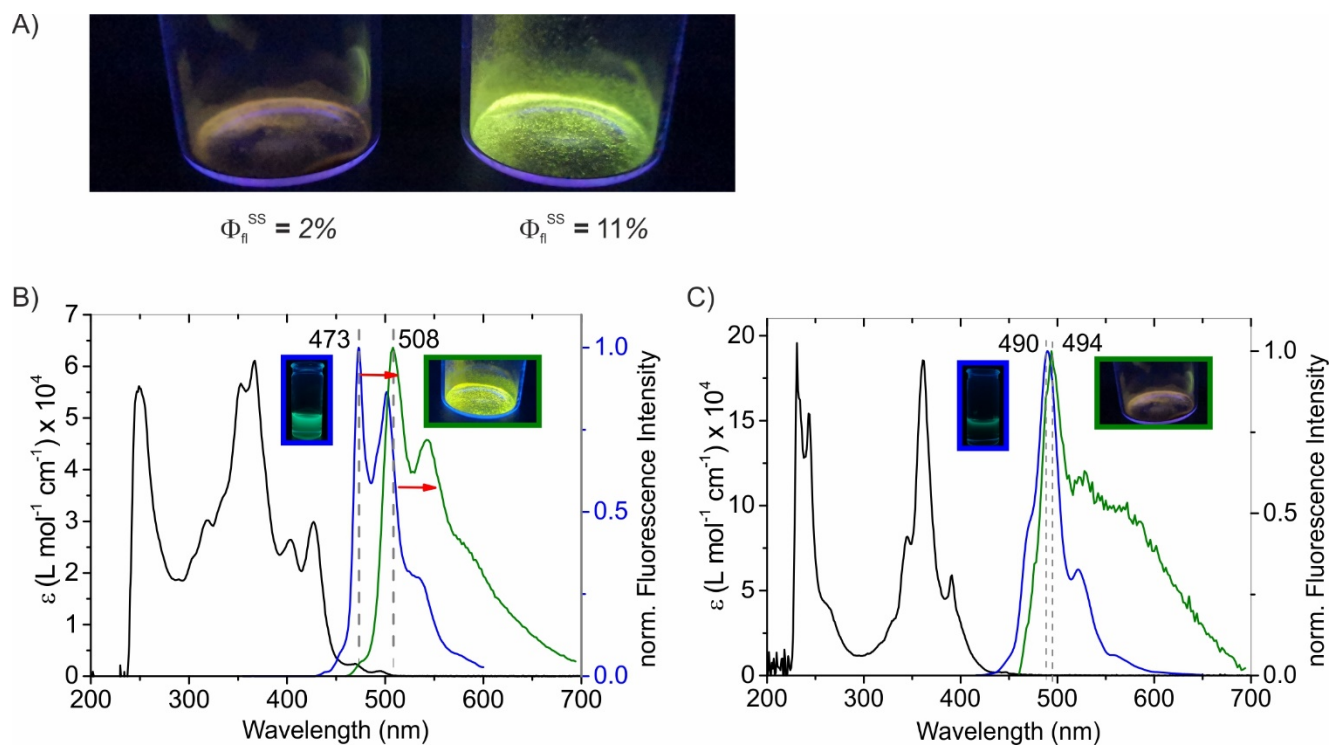


Figure S15: A) Comparison of the qualitative solid-state fluorescence of **4** (left side) and **5** (right side) under radiation of the UV lamp at 366 nm. The measured solid-state fluorescence quantum yields are given below, respectively. B and C) Comparison of the solution (blue, in DCM) and solid-state fluorescence (green) of **4** (B) and **5** (C). The absorption spectra in solution (DCM) is shown in black. The excitation wavelength was 355 nm, respectively. The solid-state fluorescence of **4** is bathochromically shifted 35 nm. The solid-state fluorescence of **5** bathochromically is shifted 4 nm. The insets show the fluorescence in solution (left, blue frame) and in solid-state (right, green frame).

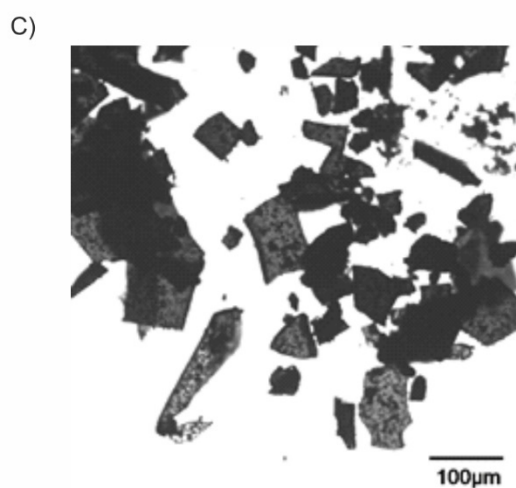
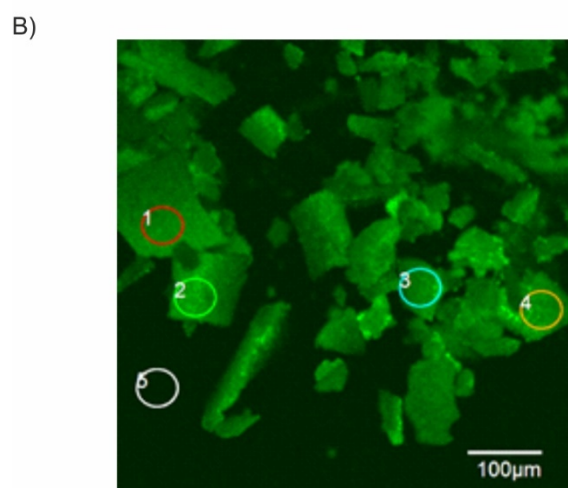
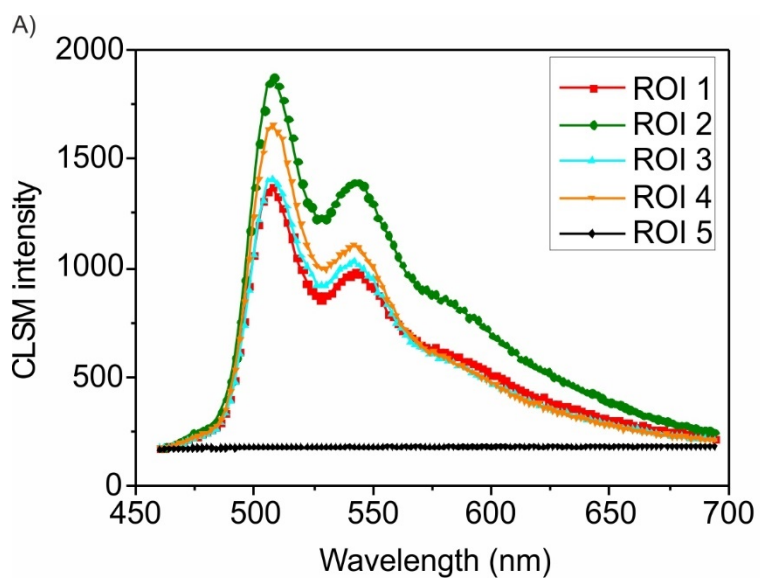


Figure S16: Spatial resolved solid state emission of **4** excited at 355 nm and at the respective region of interest (ROI) shown in B. B) Solid state emission of **4** (Exc. 355 nm; Excitation DM BS20/80; UPLSAPO 10X NA:0.40). C) Transmission image (Exc. 488 nm; 10x).

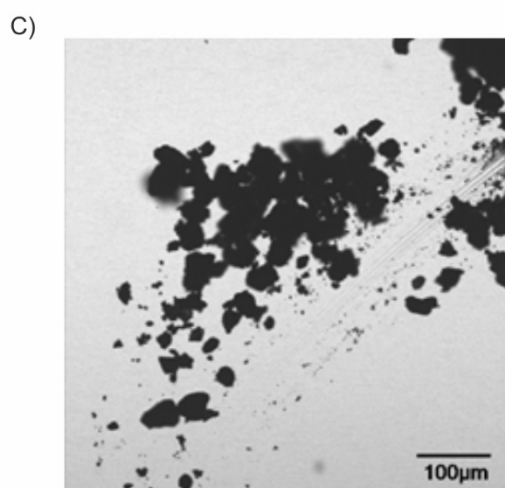
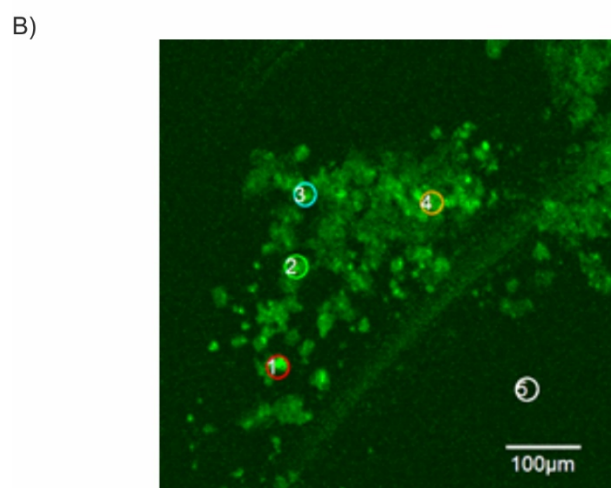
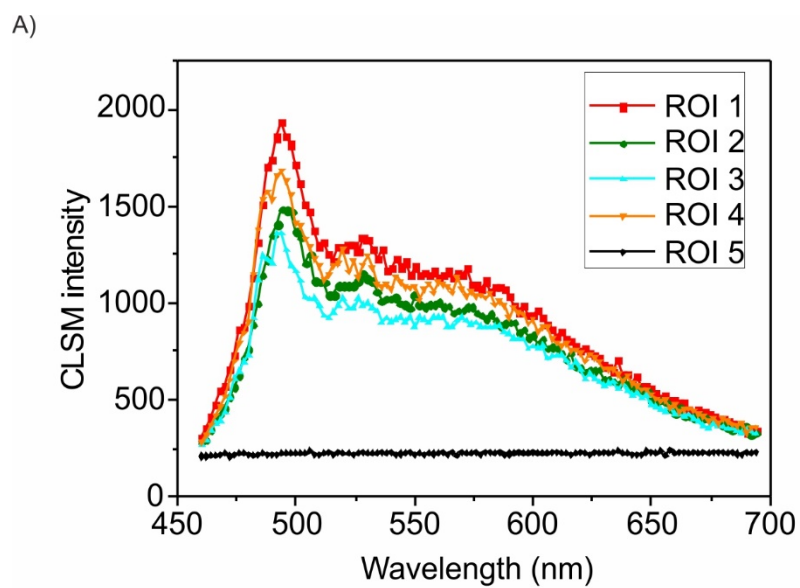


Figure S17: Spatial resolved solid state emission of **4** excited at 355 nm and at the respective ROI shown in B. B) Solid state emission of **4** (Exc. 355 nm; Excitation DM BS20/80; UPLSAPO 10X NA:0.40). C) Transmission image (Exc. 488 nm; 10x).

7. Computational Study of the racemization barrier

All calculations were performed using density functional theory (DFT) at the B3LYP/6-31G(d) level of theory in gaussian 09.^[12-13] To elucidate the racemization barrier of compound **4** we took the initial dihedral angle of 34.45° between carbon atoms C1, C7, C22 and C38 (Figure) from the crystal structure. The dihedral angle was then changed in steps of about 1° and the relaxed geometry was calculated at each dihedral angle using the Coordinate Scan within Gaussian with the keyword "Addredundant". The relative energies were calculated with respect to the energy of the crystal structure and are shown in Figure S13.

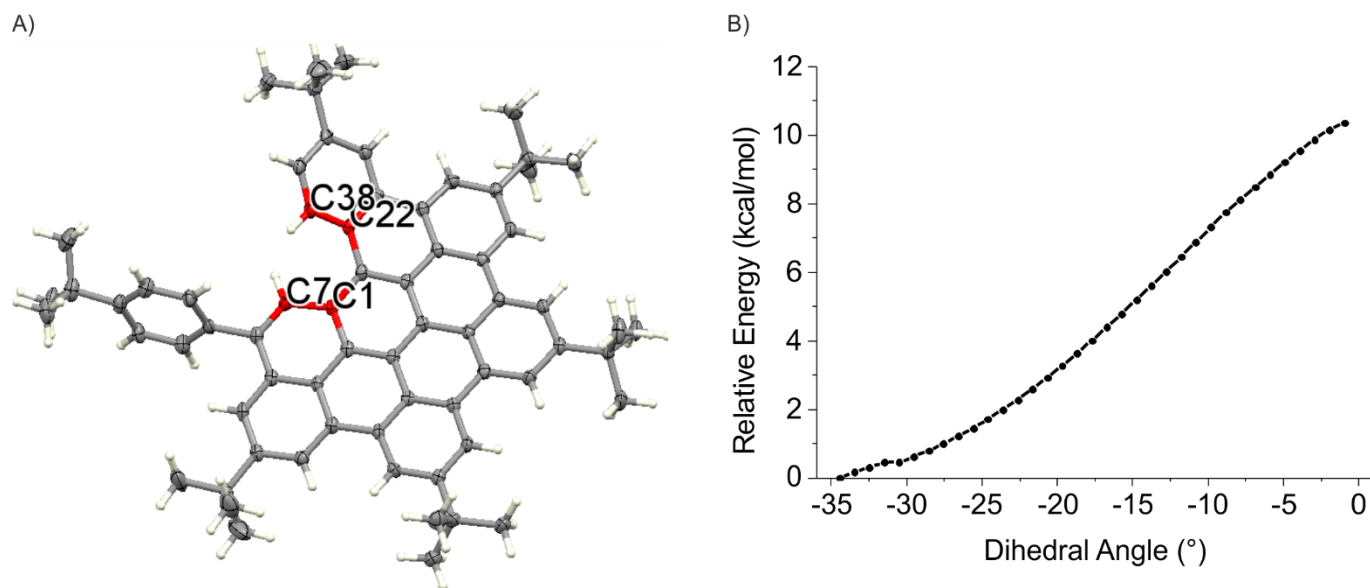


Figure S18: A) Crystal structure of **4** with the carbon atoms used for the evaluation of the racemization barrier marked in red. The dihedral angle is 34.45°. B) Calculation of the rotational barrier around the marked dihedral angle (A). The Calculation was done 1° steps from -35° to 0° using density functional theory (DFT) at the B3LYP/6-31G(d) level of theory.

To judge the accuracy of our calculations we calculated the rotational barrier of [4]helicene using our procedure. As visible in Figure S14 the rotational barrier is slightly above 4 kcal/mol and thus in accordance with the literature values.^[14-15]

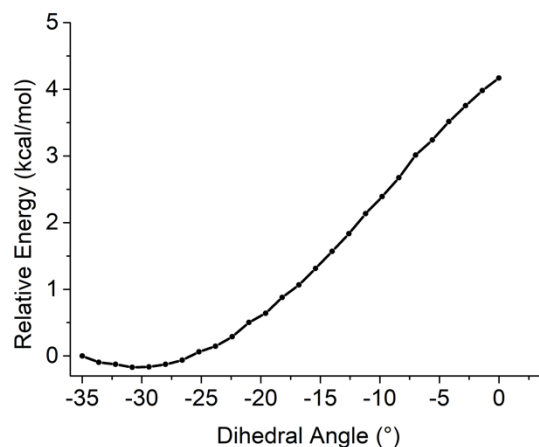


Figure S19: Calculations of the rotational barrier of [4]helicene density functional theory (DFT) at the B3LYP/6-31G(d) level of theory. The barrier is slightly above 4 kcal/mol and thus in accordance with literature values.^[14]

Notes and references

- [1] G. M. Sheldrick, *Acta Crystallogr., Sect. C: Cryst. Struct. Commun.* 2015, **71**, 3-8.
- [2] G. M. Sheldrick, *Acta Crystallogr., Sect. A: Found. Crystallogr.* 2008, **64**, 112-122.
- [3] C. B. Hubschle, G. M. Sheldrick, B. Dittrich, *J. Appl. Crystallogr.* 2011, **44**, 1281-1284.
- [4] in *APEX3*, Bruker AXS Inc., Madison, Wisconsin, USA, **2015**.
- [5] G. M. Sheldrick, *Vol. Ver. 2008/1*, University of Göttingen, Germany, **2008**.
- [6] SAINT+, Version 8.27b © ed., Bruker AXS Inc., Madison, Wisconsin, USA, **1997-2012**.
- [7] G. M. Sheldrick, Version 2014/7 ed., University of Göttingen, Germany, **2014**.
- [8] A. Gourdon, S. K. Sadhukhan, C. Viala, *Synthesis* 2003, 1521-1525.
- [9] M. H. Vilhelmsen, J. Jensen, C. G. Tortzen, M. B. Nielsen, *Eur. J. Org. Chem.* 2013, 701-711.
- [10] R. Rathore, C. L. Burns, *J. Org. Chem.* 2003, **68**, 4071-4074.
- [11] L. Zhai, R. Shukla, R. Rathore, *Org. Lett.* 2009, **11**, 3474-3477.
- [12] A. D. Becke, *J. Phys. Chem.* 1993, **98**, 5648-5652.
- [13] P. J. Stephens, F. J. Devlin, C. F. Chabalowski, M. J. Frisch, *J. Phys. Chem.* 1994, **98**, 11623-11627.
- [14] S. Grimme, S. D. Peyerimhoff, *Chem. Phys.* 1996, **204**, 411-417.
- [15] H. A. Staab, M. Diehm, C. Krieger, *Tetrahedron Lett.* 1995, **36**, 2967-2970.